Available online at www.sciencedirect.com
SCIENCE DIRECT®
PERGAMON
International Journal of Heat and Mass Transfer 46 (2003) 4097–4104
International Journal of HEAT and MASS TRANSFER
www.elsevier.com/locate/ijhmt

Numerical computation for Rayleigh–Benard convection of water in a magnetic field

Toshio Tagawa, Azusa Ujihara, Hiroyuki Ozoe *

Institute of Advanced Material Study, Kyushu University, Kasuga Koen 6-1, Kasuga 816-8580, Fukuoka, Japan

Received 15 July 2002; received in revised form 10 February 2003

Abstract

The derivation process for the model equation is shown for the natural convection of water (diamagnetic) under both gravity and magnetizing force fields and numerically solved for the Rayleigh–Benard convection in a shallow cylinder heated from below and cooled from above. The cylindrical enclosure was located at two levels in the bore of a super-conducting magnet, where the radial component of the magnetizing force is minimal and its axial component prevails. The cylindrical enclosure was assumed to be located coaxially with the bore of the magnet, and a two-dimensional model equation was presumed. Sample computations were carried out without or with a gravity force for various strengths of Rayleigh number and magnetic induction. When the enclosure was placed above the coil center, where the magnetizing force is opposed to the gravitational force, the average Nusselt number decreased with increasing strength of the magnetic field. When the enclosure was placed below the coil center, where the magnetizing force is parallel to gravity, the average Nusselt number increased above unity even at $Ra = 1000$ and 1500. All of the data agreed favorably with the classical experimental data of Silveston when plotted against the magnetic Rayleigh number proposed by Braithwaite et al.
© 2003 Elsevier Ltd. All rights reserved.

1. Introduction

Rayleigh–Benard natural convection of water has been extensively studied from laminar to turbulent flow regions in a terrestrial state. The present study examines the effect of body force exerted by a magnetic field on the Rayleigh–Benard convection of water. Recent development of a super-conducting magnet supplies large gradient of magnetic field to provide magnetizing force for any materials depending on the magnitude of magnetic susceptibility. Most materials are classified as diamagnetic, having a negative magnetic susceptibility and being repelled by a strong magnetic field. Materials with a positive magnetic susceptibility are called paramagnetic. Representative diamagnetic materials include water ($\chi_m = -9.02 \times 10^{-6}$) and bismuth ($\chi_m = -1.65 \times 10^{-4}$), and paramagnetic materials include oxygen gas ($\chi_m = 1.91 \times 10^{-6}$) and manganese ($\chi_m = 9.0 \times 10^{-4}$) [1].

According to Curie's law, the mass magnetic susceptibility χ of a paramagnetic material is inversely proportional to its absolute temperature. Thus a paramagnetic fluid convects under a gradient magnetic field if there is a temperature distribution. Magnetizing force $\vec{f}_m$ is given as follows according to Bai et al. [2].

$$\vec{f}_m = \frac{\chi_m}{2\mu_m}\vec{\nabla}b^2 = \frac{\rho\chi}{2\mu_m}\vec{\nabla}b^2 \tag{1}$$

Wakayama's group [2–6] and Kitazawa's group [7–11] have reported various new findings on the phenomena associated with magnetizing force. Tagawa and coworkers [12,13] derived model equations in similar procedure to the Boussinesq approximation for paramagnetic gases and carried out numerical computation with experimental verification.

For a diamagnetic fluid, the mass magnetic susceptibility is constant, but the magnetizing force appears due to the change of density ρ in the above Eq. (1). In

* Corresponding author. Tel.: +81-92-583-7834; fax: +81-92-583-7838.
E-mail addresses: tagawa@cm.kyushu-u.ac.jp (T. Tagawa), ozoe@cm.kyushu-u.ac.jp (H. Ozoe).

0017-9310/03/$ - see front matter © 2003 Elsevier Ltd. All rights reserved.
doi:10.1016/S0017-9310(03)00223-0

Nomenclature

$\vec{a}$	position vector on a coil $=(a, z_c)$ [m]
a	radius of a coil [m]
$\vec{A}$	$\vec{a}/h=(A, Z_c)$
$\vec{b}$	magnetic induction [T]
b_a	$\mu_m i/h$ [T]
$\vec{B}$	dimensionless magnetic induction $=\vec{b}/b_a$
C_p	specific heat at constant pressure [J/(kg K)]
d	diameter of an enclosure $=3h$ [m]
$\vec{f}_m$	magnetizing force, Eq. (1) [N/m^3]
g	gravitational acceleration [m/s^2]
h	height of a cylindrical enclosure [m]
i	electric current in a coil [A]
k	thermal conductivity of water [W/(m K)]
Nu	Nusselt number $=Q_{conv}/Q_{cond}$
p	pressure [Pa]
p'	perturbed pressure [Pa]
p_a	reference pressure $=\rho\alpha^2/h^2$ [Pa]
P	dimensionless pressure $=p'/p_a$
Pr	Prandtl number $=\nu/\alpha$
Q_{cond}	conduction heat transfer rate [J/s]
Q_{conv}	convection heat transfer rate [J/s]
r	radial coordinate [m]
$\vec{r}$	position vector in an enclosure $=(r, z)$ [m]
R	r/h
$\vec{R}$	$\vec{r}/h=(R, Z)$
Ra	Rayleigh number $=g\beta(\theta_h-\theta_c)h^3/(\alpha\nu)$
Ra_m	magnetic Rayleigh number $=Ra[1-\gamma B_z(\partial B_z/\partial Z)]$
t	time [s]
t_a	h^2/α [s]
T	dimensionless temperature $=(\theta-\theta_0)/(\theta_h-\theta_c)$
u	velocity component in a radial direction [m/s]
u_a	α/h [m/s]
U	u/u_a
w	velocity component in an axial direction [m/s]
w_a	α/h [m/s]
W	w/u_a
z	axial coordinate [m]
Z	z/h
z_c	axial position of a coil [m]
Z_c	z_c/h

Greek symbols

α	thermal diffusivity of water $=k/(\rho C_p)$ [m^2/s]
β	volumetric coefficient of expansion of water at θ_0 [1/K]
γ	$\chi b_a^2/(\mu_m g h)$
θ	absolute temperature [K]
θ_h	temperature of the hot wall [K]
θ_c	temperature of the cold wall [K]
θ_0	$(\theta_h+\theta_c)/2$ [K]
μ	viscosity of water [Pa s]
μ_m	magnetic permeability in a vacuum [H/m]
ν	kinematic viscosity of water $=\mu/\rho$ [m^2/s]
ρ	density of water [kg/m^3]
τ	dimensionless time $=t/t_a$
χ	mass magnetic susceptibility [m^3/kg]
χ_m	volumetric magnetic susceptibility $=\rho\chi$

the present study, a model equation for magnetizing force in a diamagnetic fluid such as water was derived in a similar procedure to the Boussinesq approximation, and numerical computation was carried out for the Rayleigh–Benard convection of water in a shallow cylindrical enclosure with a two-dimensional convection model.

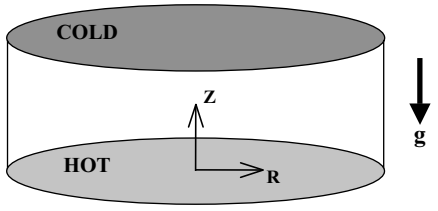

Fig. 1. Schematics of the system considered.

2. Derivation of model equation

The magnetizing force is included in the momentum equation as well as the gravitational buoyant force, as follows, for the system shown in Fig. 1.

$$\rho\,\mathrm{D}\vec{u}/\mathrm{D}t=-\vec{\nabla}p+\mu\nabla^2\vec{u}+(\rho\chi/(2\mu_m))\vec{\nabla}b^2+\rho(0,0,-g)^{\mathrm{T}} \quad (2)$$

The sign of g is negative because the z-coordinate is defined upward, against gravity. The magnetic susceptibility of water χ is negative and independent of temperature. The equation of state for water may be represented as follows.

$$\rho=\rho_0+(\partial\rho/\partial\theta)_0(\theta-\theta_0)=\rho_0-\rho_0\beta(\theta-\theta_0) \quad (3)$$

where

$$\beta=-\{(\partial\rho/\partial\theta)/\rho\}_0 \quad (4)$$

β is the volumetric coefficient of expansion due to temperature variation.

When the fluid is at a uniform temperature θ_0 the magnetizing force and the gravity force are curl-free, and no convection $\vec{u} = 0$ is resulted with $p = p_0$ and $\rho = \rho_0$. Then, Eq. (2) becomes,

$$0 = -\vec{\nabla} p_0 + \rho_0 \chi \nabla b^2/(2\mu_m) - \rho_0 g(0,0,1)^T \tag{5}$$

Subtracting Eq. (5) from Eq. (2) gives

$$\rho \mathrm{D}\vec{u}/\mathrm{D}t = -\vec{\nabla}(p - p_0) + \mu\nabla^2\vec{u} + \{\chi(\rho - \rho_0)/(2\mu_m)\}\vec{\nabla} b^2 + (\rho_0 - \rho) g(0,0,1)^T \tag{6}$$

Introducing perturbed pressure $p' = p - p_0$, where p is at a convection state and p_0 at a static state, and considering Eq. (3), we can derive the following equation.

$$\rho \mathrm{D}\vec{u}/\mathrm{D}t = -\vec{\nabla} p' + \mu\nabla^2\vec{u} - \{\rho_0\beta\chi(\theta - \theta_0)/(2\mu_m)\}\vec{\nabla} b^2 + \rho_0\beta g(\theta - \theta_0)(0,0,1)^T \tag{7}$$

Presuming $\rho \cong \rho_0$ and introducing kinematic viscosity $\nu = \mu/\rho_0$,

$$\mathrm{D}\vec{u}/\mathrm{D}t = -\vec{\nabla} p'/\rho_0 + \nu\nabla^2\vec{u} - \{\beta\chi(\theta - \theta_0)/(2\mu_m)\}\vec{\nabla} b^2 + \beta g(\theta - \theta_0)(0,0,1)^T \tag{8}$$

This leads to the following non-dimensionalized system equations, including equations of continuity, energy and Biot–Savart's law.

$$\vec{\nabla}\cdot\vec{U} = 0 \tag{9}$$

$$\mathrm{D}T/\mathrm{D}\tau = \nabla^2 T \tag{10}$$

$$\mathrm{D}\vec{U}/\mathrm{D}\tau = -\vec{\nabla} P + Pr\nabla^2\vec{U} - \gamma \cdot Ra \cdot Pr \cdot T \cdot \nabla B^2/2 + Ra \cdot Pr \cdot T \cdot (0,0,1)^T \tag{11}$$

$$\vec{B} = \frac{1}{4\pi}\oint \frac{\mathrm{d}\vec{A}\times(\vec{A} - \vec{R})}{|\vec{A} - \vec{R}|^3} \tag{12}$$

The following dimensionless variables were employed.

$$(R,Z) = (r,z)/h, \quad U = u/u_a, \quad W = w/w_a,$$
$$\tau = t/t_a, \quad P = p'/p_a, \quad \vec{B} = \vec{b}/b_a,$$
$$T = (\theta - \theta_0)/(\theta_h - \theta_c), \quad u_a = w_a = \alpha/h,$$
$$t_a = h^2/\alpha, \quad b_a = \mu_m i/h, \quad p_a = \rho\alpha^2/h^2,$$
$$Ra = g\beta(\theta_h - \theta_c)h^3/(\alpha\nu), \quad Pr = \nu/\alpha,$$
$$\gamma = \chi b_a^2/(\mu_m g h)$$

The initial conditions are as follows.

$$U = W = T = 0 \quad \text{at } \tau < 0$$

The boundary conditions are as follows.

$$U = W = 0 \quad \text{at } Z = 0, 1 \text{ and } R = 1.5$$

$$T = 0.5 \quad \text{at } Z = 0$$

$$T = -0.5 \quad \text{at } Z = 1$$

$$\partial T/\partial R = 0 \quad \text{at } R = 1.5$$

The above equations were approximated by finite difference equations and numerically solved by the HSMAC method [14]. The inertial terms were approximated by the UTOPIA scheme [15]. The grid number employed was 30×20 in radial and vertical coordinates. Symmetry about the cylinder axis was assumed, since the magnetic coil is placed coaxially with the cylindrical enclosure.

3. Model systems and computed result

Model systems are shown in Fig. 2. The vertical cylinder is placed either at 56.3 mm above the coil (position 1) or 56.3 mm below the coil (position 2) for the cylindrical enclosure of 15 mm in height and 45 mm in diameter. The radius of the electric coil is 90 mm. This combination of sample dimensional values for geometry defines the strength of the magnetic field uniquely. In this system the enclosure is assumed to be placed inside the bore space of a super-conducting magnet.

3.1. Effect of grid numbers

Numerical computations were carried out with finite difference approximation, and some truncation error may be included. To estimate its magnitude, sample computations were carried out for position 1, at $Ra = 7000$ and $Pr = 6$ for three cases of $\gamma = 0, -600$ and -1000.

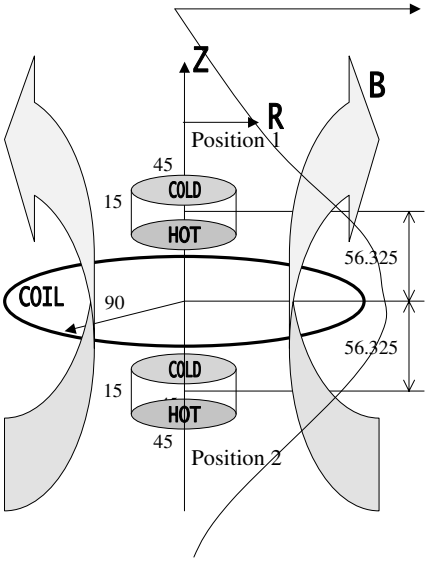

Fig. 2. Location of enclosure in the bore space of a super-conducting magnet.

Table 1
Effect of grid numbers on the average Nusselt number for position 1, $Ra = 7000$, $Pr = 6$

γ	Computed with 30×20 grids in $r\times z$ coordinates	Computed with 60×40 grids in $r\times z$ coordinates	Relative error
0	2.081	2.044	0.018
−600	1.738	1.714	0.014
−1000	1.336	1.321	0.011

Grid numbers of 30×20 and 60×40 in the radial and vertical coordinates were also tested. The results are listed in Table 1. The maximum difference is 1.8%, and we selected grid numbers 30×20 for subsequent computations, since the main concern of this report is to clarify the general effect of magnetic field on the Rayleigh–Benard convection of water rather than determine accurate numerical values of the average Nusselt number.

3.2. Computed result for the system without gravity

For the system without gravitational acceleration, we can see the effect of magnetizing force alone. Transient computation converged smoothly. For the system at $g = 0$, γ becomes infinity and Ra becomes zero, but the system can be defined with finite values of γRa. Table 2 shows the converged values of the average Nusselt number. If the temperature difference between the hot and cold walls is 10 K, the magnetic induction at the center of the enclosure is 0.923 T for $\gamma Ra = -7.0\times10^6$ and 0.653 T for $\gamma Ra = -3.5\times10^6$. Fig. 3 shows computed isothermal contours and velocity vectors for positions 1 and 2 at $Pr = 6$ without gravitational acceleration. At position 1, the magnetizing force acts in the positive Z-direction, and the water layer in a cylinder heated from below and cooled from above approaches the conduction state. In (i), the velocity vectors are drawn on a scale of 100 times larger than those in (ii) and (iii) for easy visualization. The actual absolute velocity is almost zero, and a quasi-conduction state is attained. On the other hand, at position 2, the magnetizing force acts downward in the Z-direction, and the magnetizing force acts to give larger Nusselt number with the increase in $|\gamma Ra|$.

According to the derivation of the model equation, this can be explained in another way as follows. Water near a hot wall has lower density and is less repelled by the magnetic field than that near a cold wall. Therefore, at position 1, water receives less accelerating force with the increase of $|\gamma Ra|$, but at position 2, water is unstable and convection results if $|\gamma Ra|$ is more than critical state.

Table 2
Computed results for $g = 0$ and $Pr = 6$ and equivalent dimensional value of the system in Fig. 2

Position	γRa	Ra_m	$Nu_{ave.}$	$\Delta\theta$ [K]	$b_z\|_{center}$ [T]
1	-7.0×10^6	−4121	1.000	10	0.923
2	-2.9×10^6	1708	1.0008	10	0.594
	-3.5×10^6	2061	1.063	10	0.653
	-7.0×10^6	4121	1.674	10	0.923

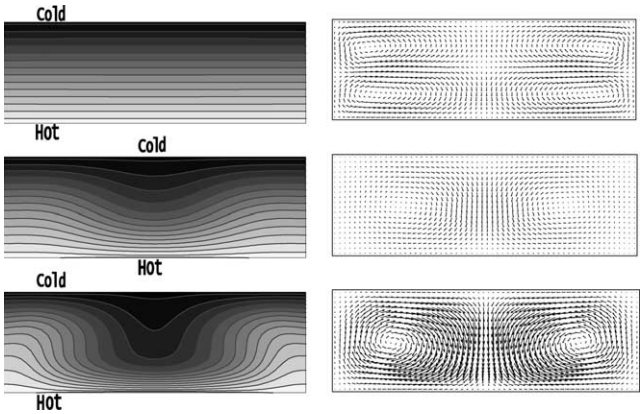

Fig. 3. Computed isotherms (left) and velocity vectors (right) in a cross section of a vertical shallow cylindrical enclosure without gravitational acceleration but with a magnetic field for $Pr = 6$: (i) position 1, $\gamma Ra = -7.0\times10^6$, $Nu = 1.000$; (ii) position 2, $\gamma Ra = -3.5\times10^6$, $Nu = 1.063$; (iii) position 2, $\gamma Ra = -7.0\times10^6$, $Nu = 1.674$.

Table 3
List of average Nusselt number at positions 1 and 2 for $Pr = 6$ under a gravity field

γ	Ra_m/Ra at position 1	Average Nusselt number at position 1			Ra_m/Ra at position 2	Average Nusselt number at position 2		
		$Ra = 3000$	$Ra = 7000$	$Ra = 12000$		$Ra = 1000$	$Ra = 1500$	$Ra = 3000$
0	1.000	4.393	2.081	2.463	1.000	1.000	1.000	1.393
−200	0.882	1.278	1.973	2.343	1.118	1.000	1.000	1.493
−400	0.764	1.150	1.866	2.245	1.236	1.000	1.000	1.581
−600	0.647	1.024	1.738	2.129	1.353	1.000	1.054	1.659
−800	0.529	1.000	1.565	1.985	1.471	1.000	1.119	1.729
−1000	0.411		1.336	1.796	1.589	1.000	1.184	
−1200	0.293		1.059	1.495	1.707	1.000	1.248	
−1300	0.235		1.000	1.290	1.765			
−1400	0.176		1.000	1.070	1.824	1.000		
−1500	0.117		1.000	1.000	1.883	1.002		
−1600	0.058			1.000	1.942	1.023		
−1698	0.000				2.000			
−1800					2.060	1.064		
−2000					2.178	1.107		
−2200					2.295	1.151		

3.3. Computed result for the system in a gravity field

Numerical computations were then carried out for the system placed in a gravity field. Transient computation again converged smoothly with the converged values of the average Nusselt numbers as listed in Table 3. These are also plotted in Fig. 4(a) for position 1 and Fig. 4(b) for position 2. For position 1, when the strength $|\gamma|$ of the magnetic field is increased, the average Nusselt number decreases toward the conduction state of $Nu = 1$ with the increase of $|\gamma|$ for any Rayleigh number $Ra = 3000$, 7000, 12 000 as shown in Table 2. This means that the system of position 1 tends to a state of no acceleration (equivalent to micro-gravity state) with increase in the strength of magnetic field.

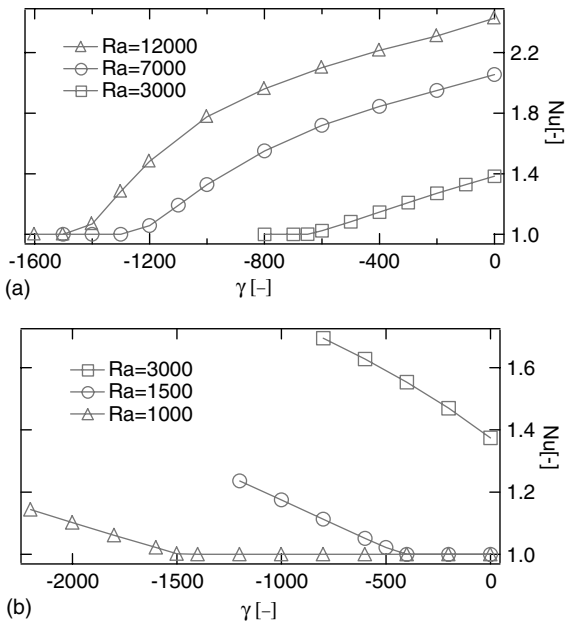

Fig. 4. Summary of computed average Nusselt numbers for $Pr = 6$ versus the strength of magnetic field γ with a parameter of Rayleigh number: (a) position 1 and (b) position 2.

Fig. 4(b) for position 2 shows that the average Nusselt number increases with the strength $|\gamma|$ of magnetic field even for Rayleigh numbers $Ra = 1000$ and 1500, which are less than the critical value of $Ra = 1708$. This is because the magnetizing force acts to assist the gravitational driving force. For $Ra = 3000$, the average Nusselt number increases with $|\gamma|$, suggesting the enhancement of convection and heat transfer rate due to the magnetizing force.

Fig. 5 shows computed isothermal contours for position 1 at (a) $Ra = 3000$ and (b) $Ra = 12000$. The magnitude of γ for (a) is 0, −400 and −800 downward, and that for (b) is 0, −800 and −1600 downward. At position 1, the direction of magnetizing force vector is upward, as shown at the right-hand side of graphs, and the net acceleration decreases with the increase in $|\gamma|$. The conduction state, $Nu = 1.000$, is finally attained for any value of the Rayleigh number. On the other hand, at position 2, the magnetizing force acts to assist the acceleration with the increase in $|\gamma|$, and the Rayleigh–Benard convection is enhanced, as shown in Fig. 6.

4. Discussion

Braithwaite et al. [16] reported the experimental Nusselt number for aqueous solutions of gadolinium nitrate (paramagnetic) in a magnetic field and proposed the magnetic Rayleigh number, Ra_m. This represents an effective Rayleigh number for Rayleigh–Benard natural

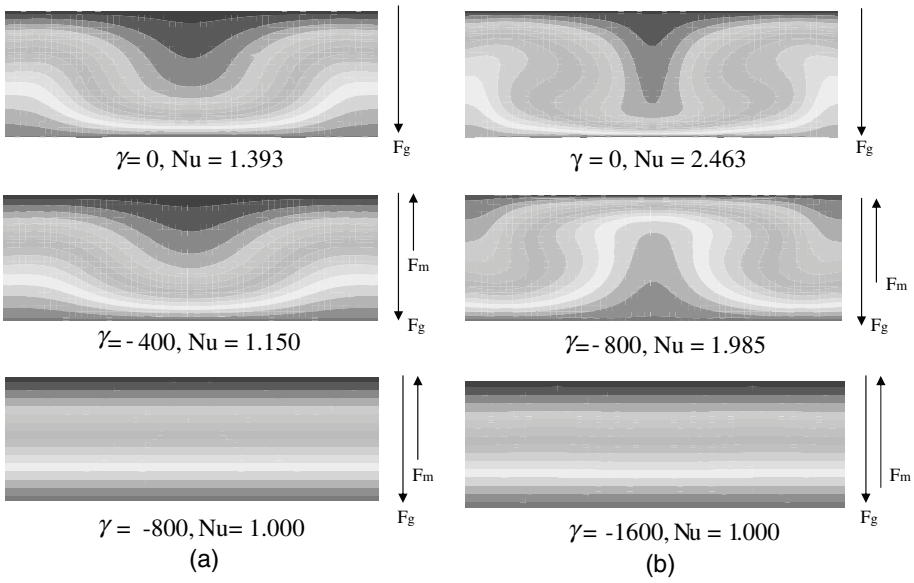

Fig. 5. Computed isothermal contours at position 1 and $Pr = 6$: (a) $Ra = 3000$ and (b) $Ra = 12000$.

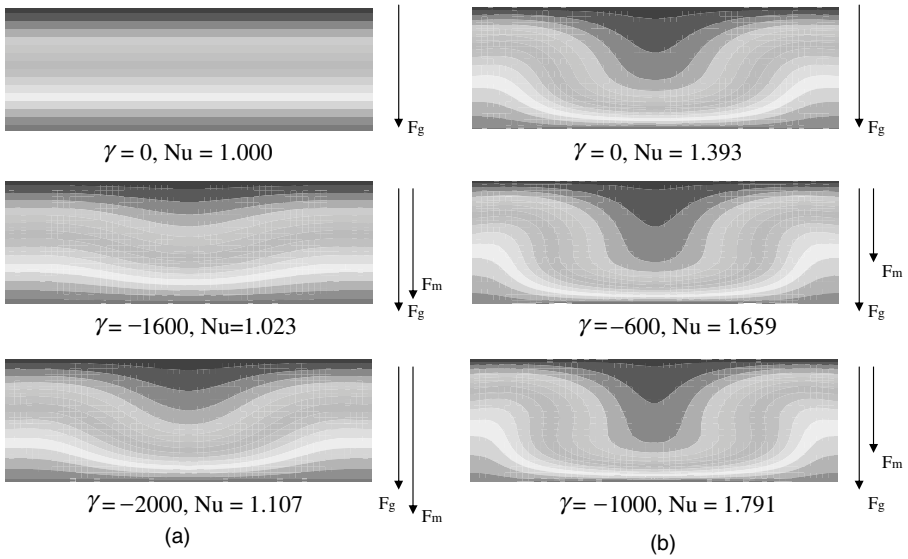

Fig. 6. Computed isothermal contours at position 2 and $Pr = 6$: (a) $Ra = 1000$ and (b) $Ra = 3000$.

convection. It is derived as a summation of gravitational buoyant force and the magnetic induced buoyant force terms in the Z-directional momentum equation, as follows, from Eq. (11).

$$fm_z = -\gamma RaPrT(\partial/\partial Z)(B^2/2) + RaPrT$$
$$= -\gamma RaPrT(\partial/\partial Z)(B_r^2 + B_\phi^2 + B_Z^2)/2 + RaPrT$$

In the present system in which the enclosure is located inside the bore space of a super-conducting magnet, the circumferential component of the magnetic induction, B_ϕ, is zero, since the center of the coil is coincident with the axis of the enclosure and $\partial Br^2/\partial Z \cong 0$ at ± 56.3 mm height. Thus, we get

$$fm_z = RaPrT(1 - \gamma B_Z(\partial B_Z/\partial Z)) = Ra_{\mathrm{m}}PrT$$

From this we get the magnetic Rayleigh number.

$$Ra_{\mathrm{m}} = Ra(1 - \gamma B_Z(\partial B_Z/\partial Z))$$

The magnetic Rayleigh numbers are tabulated in Table 3 corresponding to the value of γ, since B_Z and $(\partial B_Z/\partial Z)$

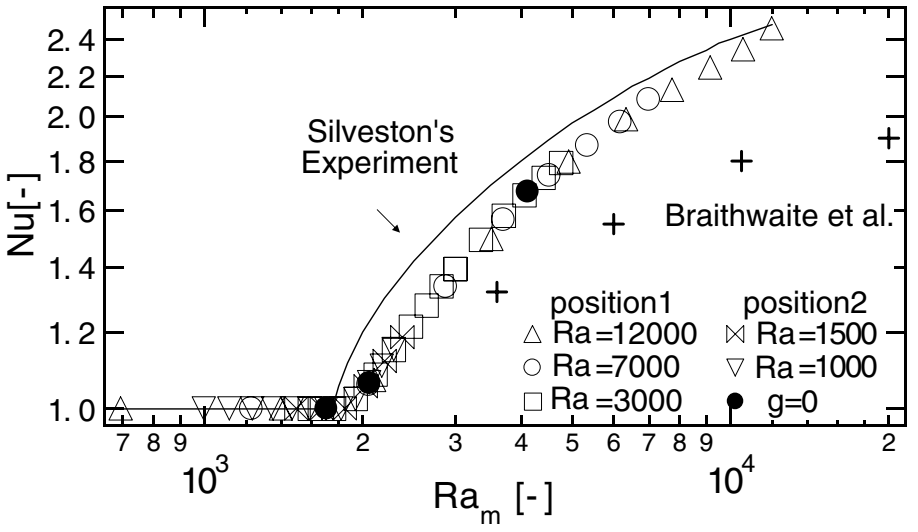

Fig. 7. Summary of computed average Nusselt number of water in a shallow cylinder heated from below and cooled from above and located at position 1, position 2 or without gravitational acceleration, versus the magnetic Rayleigh number. $Pr = 6$. Silveston's data [18], Braithwaite et al. [16].

are fixed for the present system of Fig. 1 at the center of the enclosure as $B_Z = 0.05076$ and $(\partial B_Z/\partial Z) = 0.0116$, as computed from Eq. (12).

This magnetic Rayleigh number was also employed to correlate the Rayleigh–Benard convection of air in a magnetic field by Maki et al. [17] and was confirmed to be appropriate in scale.

The computed average Nusselt numbers are all plotted versus Ra_m for the system without and with a gravity force and for positions 1 and 2 in Fig. 7. The experimental data of Silveston [18] are also plotted with a solid line for comparison. The computed average Nusselt numbers are slightly smaller than the experimental data, which were obtained for a very shallow layer. The present enclosure has diameter/height = 3, and the slightly smaller Nusselt number may be reasonable. The experimental data of Braithwaite et al. are also plotted, though they differ from the curve of Silveston.

5. Conclusion

The Rayleigh–Benard convection of water (diamagnetic fluid) in a cylindrical enclosure placed in a bore space of a super-conducting magnet was considered as a model. A model equation of convection due to magnetizing force was derived by a similar process to the Boussinesq approximation for buoyancy convection. The model equations were numerically solved for two locations of the enclosure in the bore space of a super-conducting magnet: above (position 1) and below (position 2) the coil center. These two locations were selected to have the minimum radial component of the magnetizing force. At position 1, the direction of the magnetizing force is against gravity and the average Nusselt number converges to unity with $|\gamma|$, which represents the strength of magnetic field. At position 2, the direction of the magnetizing force is downward, parallel to the gravity force, and the average Nusselt number increases and convection occurs even for Rayleigh numbers less than the critical value of 1708. These Nusselt numbers are plotted against the magnetic Rayleigh number Ra_m reported by Braithwaite et al. to reveal a good agreement with the classical experimental data of Silveston, although the experimental data of Braithwaite et al. differ from those of Silveston.

References

[1] M. Kato, Electromagnetics, University of Tokyo Press, 1986, p. 150 (in Japanese).
[2] B. Bai, A. Yabe, J. Qi, N.I. Wakayama, Quantitative analysis of air convection caused by magnetic-fluid coupling, AIAA J. 37 (12) (1999) 1538–1543.
[3] N.I. Wakayama, Behavior of flow under gradient magnetic fields, J. Appl. Phys. 69 (4) (1991) 2734–2736.
[4] N.I. Wakayama, Effect of a decreasing magnetic field on the flow of nitrogen gas, Chem. Phys. Lett. 185 (5–6) (1991) 449–451.
[5] N.I. Wakayama, Magnetic promotion of combustion in diffusion flames, Combust. Flame 93 (3) (1993) 207–214.
[6] N.I. Wakayama, H. Ito, Y. Kuroda, O. Fujita, K. Ito, Magnetic support of combustion in diffusion flames under microgravity, Combust. Flame 107 (1–2) (1996) 187–192.
[7] Y. Ikezoe, N. Hirota, J. Nakagawa, K. Kitazawa, Making water levitate, Nature 393 (1998) 749–750.

[8] Y. Ikezoe, N. Hirota, T. Sakihama, K. Mogi, H. Uetake, T. Homma, J. Nakagawa, H. Sugawara, K. Kitazawa, Acceleration effect on the rate of dissolution of oxygen in a magnetic field, J. Jpn. Inst. Appl. Magn. 22 (4-2) (1998) 821–824 (in Japanese).

[9] K. Kitazawa, N. Hirota, Y. Ikezoe, H. Uetake, Novel magnetic field effects on non-magnetic substances: Moses effect, magneto-Archimedes levitation, magneto-enhanced vaporization and oxygen dissolution into water, in: Proceedings of the Third International Symposium on Electromagnetic Processing of Materials, Nagoya, 2000, pp. 9–13.

[10] J. Nakagawa, N. Hirota, K. Kitazawa, M. Shoda, Magnetic field enhancement of water vaporization, J. Appl. Phys. 86 (5) (1999) 2923–2925.

[11] H. Uetake, J. Nakagawa, N. Hirota, K. Kitazawa, Nonmechanical magnetothermal wind blower by a superconducting magnet, J. Appl. Phys. 85 (8) (1999) 5735–5737.

[12] T. Tagawa, R. Shigemitsu, H. Ozoe, Magnetizing force modeled and numerically solved for natural convection of air in a cubic enclosure: effect of the direction of the magnetic field, Int. J. Heat Mass Transfer 45 (2002) 267–277.

[13] M. Kaneda, T. Tagawa, H. Ozoe, Convection induced by a cusp-shaped magnetic field for air in a cube heated from above and cooled from below, J. Heat Transfer 124 (2002) 17–25.

[14] C.W. Hirt, B.D. Nichols, N.C. Romero, A numerical solution algorithm for transient fluid flow, Los Alamos Scientific Laboratory, LA-5852, 1975.

[15] T. Tagawa, H. Ozoe, Effect of Prandtl number and computational schemes on the oscillatory natural convection in an enclosure, Numer. Heat Transfer, Part A 30 (2) (1996) 271–282.

[16] D. Braithwaite, E. Beaugnon, R. Tournier, Magnetically controlled convection in a paramagnetic fluid, Nature 354 (14) (1991) 134–136.

[17] S. Maki, T. Tagawa, H. Ozoe, Enhanced convection or quasi-conduction states measured in a super-conducting magnet for air in a vertical cylindrical enclosure heated from below and cooled from above in a gravity field, J. Heat Transfer 124 (4) (2002) 667–673.

[18] P.L. Silveston, Wärmedurchgang in waagerechten Flussigkeitsschichten, Part 1, Forch. Ing. Wes. (24), 1958, pp. 29–32, 59–69.